

Electronic Supplementary Information

**Bioorthogonal Control of the Phosphorescence and Singlet Oxygen  
Photosensitisation Properties of Iridium(III) Tetrazine Complexes†**

Peter Kam-Keung Leung,<sup>a</sup> Lawrence Cho-Cheung Lee,<sup>a</sup> Herman Ho-Yin Yeung,<sup>a</sup> Kai-Wa Io,<sup>a</sup>  
and Kenneth Kam-Wing Lo<sup>\*abc</sup>

<sup>a</sup> Department of Chemistry, City University of Hong Kong, Tat Chee Avenue, Kowloon, Hong Kong, P. R. China

<sup>b</sup> State Key Laboratory of Terahertz and Millimetre Waves, City University of Hong Kong, Tat Chee Avenue, Kowloon, Hong Kong, P. R. China

<sup>c</sup> Centre of Functional Photonics, City University of Hong Kong, Tat Chee Avenue, Kowloon, Hong Kong, P. R. China

## Table of Contents

<b>Experimental</b>	S5
<b>Table S1</b>	Electronic absorption spectral data of complexes <b>1 – 4</b> and bpy-Tz-Ph in CH <sub>2</sub> Cl <sub>2</sub> and CH <sub>3</sub> CN at 298 K. S24
<b>Table S2</b>	Photophysical data of complexes <b>1 – 4</b> . S25
<b>Table S3</b>	Lipophilicity (log $P_{o/w}$ ) and solubility of complexes <b>1 – 4</b> at 298 K. S26
<b>Table S4</b>	FRET parameters of complexes <b>1 – 4</b> . S27
<b>Table S5</b>	Electrochemical data of complexes <b>1 – 4</b> and bpy-Tz-Ph. S28
<b>Table S6</b>	Electrochemical data of complexes <b>1b – 4b</b> and bpy-TCO-Ph. S29
<b>Table S7</b>	Second-order rate constants ( $k_2$ ) of complexes <b>1 – 4</b> and bpy-Tz-Ph upon reactions with <b>BCN-OH</b> and <b>TCO-OH</b> in a mixture of MeOH/H <sub>2</sub> O (1:1, v/v) at 298 K. S30
<b>Table S8</b>	<sup>1</sup> O <sub>2</sub> generation quantum yields ( $\Phi_{\Delta}$ ) of complexes <b>1 – 4</b> , <b>1a – 4a</b> and <b>1b – 4b</b> in aerated CH <sub>3</sub> CN at 298 K. DPBF was used as the <sup>1</sup> O <sub>2</sub> scavenger. S31
<b>Table S9</b>	Cytotoxicity of complex <b>2</b> towards transfected HeLa cells in the dark and upon irradiation at 365 nm for 5 min. PI is the ratio of IC <sub>50,dark</sub> /IC <sub>50,light</sub> under different conditions. S32
<b>Table S10</b>	Cellular uptake of complexes <b>1 – 4</b> by HeLa cells transfected with the pHTN HaloTag CMV-neo Vector. S33
<b>Fig. S1</b>	Electronic absorption spectra of complexes <b>1 – 4</b> and bpy-Tz-Ph in CH <sub>2</sub> Cl <sub>2</sub> (black) and CH <sub>3</sub> CN (red) at 298 K. S34

<b>Fig. S2</b>	Emission spectra of complexes <b>1 – 4</b> in degassed CH <sub>2</sub> Cl <sub>2</sub> (black) and CH <sub>3</sub> CN (red) at 298 K. Excitation wavelength = 350 nm.	S35
<b>Fig. S3</b>	Relative absorbance of solutions of complexes <b>1 – 4</b> (black), <b>1a – 4a</b> (red) and <b>1b – 4b</b> (blue) (10 μM) in aerated potassium phosphate buffer (50 mM, pH 7.4)/DMSO (99:1, v/v) at 298 K under continuous photoexcitation at 365 nm (1 mW/cm <sup>2</sup> ).	S36
<b>Fig. S4</b>	Relative emission intensities of solutions of complexes <b>1 – 4</b> (black), <b>1a – 4a</b> (red) and <b>1b – 4b</b> (blue) (10 μM) in aerated potassium phosphate buffer (50 mM, pH 7.4)/DMSO (99:1, v/v) at 298 K under continuous photoexcitation at 365 nm (1 mW/cm <sup>2</sup> ).	S37
<b>Fig. S5</b>	Latimer diagrams showing the excited-state redox potentials of complexes <b>1 – 4</b> .	S38
<b>Fig. S6</b>	Latimer diagrams showing the excited-state redox potentials of complexes <b>1b – 4b</b> .	S39
<b>Fig. S7</b>	Spectral overlap of the absorption spectrum of the acceptor bpy-Tz-Ph and normalized emission spectrum of the donor complexes <b>1 – 4</b> in CH <sub>3</sub> CN at 298 K. The extinction coefficient of bpy-Tz-Ph was 425 M <sup>-1</sup> cm <sup>-1</sup> at 540 nm.	S40
<b>Fig. S8</b>	Pseudo first-order kinetics for the reactions of complexes <b>1 – 4</b> with <b>BCN-OH</b> at different concentrations in MeOH/H <sub>2</sub> O (1:1, v/v) at 298 K. The slope corresponds to the <i>k</i> <sub>2</sub> of the reaction.	S41

<b>Fig. S9</b>	Pseudo first-order kinetics for the reactions of complexes <b>1 – 4</b> with <b>TCO-OH</b> at different concentrations in MeOH/H <sub>2</sub> O (1:1, v/v) at 298 K. The slope corresponds to the $k_2$ of the reaction.	S42
<b>Fig. S10</b>	SDS-PAGE analysis of the reactions of complex <b>2</b> with <b>BCN-BSA</b> and <b>TCO-BSA</b> . Left: UV transillumination; right: Coomassie Blue staining. Lanes 1 and 4: complex with <b>BCN-BSA</b> ; lanes 2 and 5: complex with <b>TCO-BSA</b> ; lanes 3 and 6: complex with unmodified BSA.	S43
<b>Fig. S11</b>	LSCM images of HeLa cells pretreated with <b>BCN-morph</b> (50 $\mu$ M, 2 h) and <b>BCN-DPPE</b> (50 $\mu$ M, 2h) and incubated with complex <b>2</b> (10 $\mu$ M, 2 h) at 37°C.	S44
<b>Fig. S12</b>	LSCM images of HeLa cells incubated with complex <b>2</b> (10 $\mu$ M) at 37°C for 1 h. Only cells expressing cytoplasm-enriched HaloTag with pretreatment of <b>BCN-C6-Cl</b> (50 $\mu$ M, 1 h) showed intense phosphorescence signal.	S45
<b>References</b>		S46

## Experimental

### Materials and Synthesis

All solvents were of analytical reagent grade and purified according to published procedures.<sup>1</sup> All buffer components were of biological grade and used as received. Autoclaved Milli-Q water was used for the preparation of the aqueous solutions. 2-(2,4-Difluorophenyl)pyridine (Hdfppy), 2-phenylpyridine (Hppy), 2-phenylquinoline (Hpq), 2-phenylquinoline-4-carboxylic Acid (Hpqa), IrCl<sub>3</sub>·nH<sub>2</sub>O, selenium dioxide, 1,4-dioxane, hydroxylamine hydrochloride, formic acid, benzonitrile, sulfur, hydrazine monohydrate, sodium nitrite, 2-(2-*tert*-butoxycarbonylaminoethoxy)ethanol, 6-chloro-1-iodohexane, tetrabutylammonium hexafluorophosphate (TBAP), Na<sub>2</sub>S<sub>2</sub>O<sub>5</sub>, Na<sub>2</sub>CO<sub>3</sub>, NH<sub>4</sub>OH, MgSO<sub>4</sub>, KPF<sub>6</sub>, AgNO<sub>3</sub>, Et<sub>3</sub>N, NaCl and octan-1-ol were purchased from Acros. 4,4'-Dimethyl-2,2'-bipyridine, (1*R*,8*S*,9*s*)-bicyclo[6.1.0]non-4-yn-9-ylmethanol (**BCN-OH**), (1*R*,8*S*,9*s*)-bicyclo[6.1.0]non-4-yn-9-ylmethyl-*N*-succinimidyl carbonate (**BCN-NHS**), 4-(2-aminoethyl)morpholine, 1,2-dipalmitoyl-*sn*-glycero-3-phosphoethanolamine (DPPE), 3-(4,5-dimethylthiazol-2-yl)-2,5-diphenyltetrazolium bromide (MTT), 1,3-diphenylisobenzofuran (DPBF), phenalenone and [Ru(bpy)<sub>3</sub>]Cl<sub>2</sub> was supplied by Sigma-Aldrich. *trans*-Cyclooct-4-en-1-ol (**TCO-OH**) and *trans*-cyclooct-4-enyl 2,5-dioxo-1-pyrrolidinyl carbonate (**TCO-NHS**) were obtained from BroadPharm. Bovine serum albumin (BSA) was purchased from Calbiochem and used as received. The pHTN HaloTag CMV-neo Vector was supplied by Promega. PD-10 size-exclusion columns and YM-10 microcon filters were obtained from GE Healthcare and Millipore, respectively. Novex sharp pre-stained protein standard, Dulbecco's modified Eagle's medium (DMEM), phenol red-free DMEM, fetal bovine serum (FBS), penicillin/streptomycin, 10X phosphate-buffered saline (PBS), trypsin-EDTA, Opti-MEM, Lipofectamine 3000, LysoTracker

Deep Red and ER-Tracker Green were purchased from Invitrogen. HeLa cells were obtained from American Type Culture Collection. Unless otherwise specified, the growth medium for cell culture contained DMEM with 10% FBS and 1% penicillin/streptomycin. Methyl 2-phenyl-4-quinolinecarboxylate (Hpqe),<sup>2</sup> the iridium(III) dimers  $[\text{Ir}_2(\text{N}^{\wedge}\text{C})_4\text{Cl}_2]$  ( $\text{HN}^{\wedge}\text{C}$  = Hdfppy, Hppy, Hpq and Hpqe),<sup>3</sup> 4-carboxylaldehyde-4'-methyl-2,2'-bipyridine (bpy-CHO),<sup>4</sup> *N*-[(1*R*,8*S*,9*S*)-bicyclo[6.1.0]non-4-yn-9-ylmethyloxycarbonyl]-4-(2-aminoethyl)morpholine (**BCN-morph**),<sup>5</sup> ((1*R*,8*S*,9*S*)-bicyclo[6.1.0]non-4-yn-9-yl)methyl (2-(2-((6-chlorohexyl)oxy)ethoxy)ethyl)carbamate (**BCN-C6-Cl**)<sup>6</sup> and *trans*-cyclooct-4-en-1-yl (2-(2-((6-chlorohexyl)oxy)ethoxy)ethyl)carbamate (**TCO-C6-Cl**)<sup>6</sup> were prepared by reported methods.

### Physical Measurements and Instrumentation

<sup>1</sup>H and <sup>13</sup>C NMR spectra were recorded on Bruker 300, 400 and 600 MHz AVANCE III spectrometers at 298 K using deuterated solvents. Chemical shifts ( $\delta$ , ppm) were reported relative to tetramethylsilane (TMS). Positive-ion electrospray ionization (ESI) mass spectra were recorded on a AB Sciex API 3200 QTRAP mass spectrometer at 298 K. Infrared (IR) spectra of the samples in KBr pellets were recorded in the range of 4000 – 400 cm<sup>-1</sup> using a Perkin Elmer Spectrum 100 FTIR spectrometer. Elemental analyses were carried out on an Elementar Analysensysteme GmbH Vario MICRO elemental analyzer.

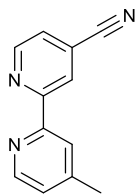
The electrochemical measurements were performed on a CH Instruments Electrochemical Workstation CHI750A. Cyclic voltammetry experiments were carried out at RT using a two-compartment glass cell with a working volume of 500  $\mu\text{L}$ . A platinum gauze counter electrode

was accommodated in the working electrode compartment. The working and reference electrodes were a glassy carbon electrode and a Ag/AgNO<sub>3</sub> (0.1 M TBAP in CH<sub>3</sub>CN) electrode, respectively. The reference electrode compartment was connected to the working electrode compartment via a Luggin capillary. Solutions for electrochemical measurements were degassed with prepurified nitrogen gas. All potentials were referred to SCE.

Electronic absorption spectra were recorded on an Agilent 8453 diode array spectrophotometer. Steady-state emission spectra were recorded on a HORIBA Jobin Yvon FluoroMax-4 spectrofluorometer. Unless specified otherwise, all solutions for photophysical studies were degassed with no fewer than four successive freeze-pump-thaw cycles and stored in a 10-cm<sup>3</sup> round bottomed flask equipped with a side-arm 1-cm fluorescence cuvette and sealed from the atmosphere by a Rotaflo HP6/6 quick-release Teflon stopper. Luminescence quantum yields were measured by the optically dilute method<sup>7</sup> using an aerated aqueous solution of [Ru(bpy)<sub>3</sub>]Cl<sub>2</sub> ( $\Phi_{em} = 0.028$ ,  $\lambda_{ex} = 455$  nm) as the standard solution.<sup>8</sup> The concentrations of the standard and sample solutions were adjusted until the absorbance at 455 nm was 0.1. The emission lifetimes were measured on a Edinburgh Instruments LP920-KS Laser Flash Photolysis spectrometer in the kinetic mode with the 355 nm output of the Spectra-Physics Quanta-Ray Lab-150 pulsed Nd:YAG laser as the excitation source.

## Synthesis

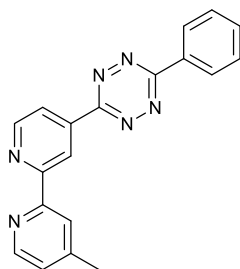
bpy-CN



A mixture of bpy-CHO<sup>4</sup> (500 mg, 2.53 mmol) and hydroxylamine hydrochloride (227 mg, 3.27 mmol) in formic acid (10 mL) was refluxed under an inert atmosphere of nitrogen for 18 h. The resulting solution was neutralized with Na<sub>2</sub>CO<sub>3</sub> at room temperature and extracted with CH<sub>2</sub>Cl<sub>2</sub> (30 mL × 3). The combined organic extract was dried over MgSO<sub>4</sub> and evaporated to dryness yielding a white solid, which was purified by column chromatography on silica gel. The desired product was eluted with CH<sub>2</sub>Cl<sub>2</sub>. The solvent was removed under reduced pressure to afford the product as a white solid. Yield: 394 mg (80%). <sup>1</sup>H NMR (300 MHz, CDCl<sub>3</sub>, 298 K): δ 8.85 (d, 1H, *J* = 4.8 Hz, H6 of bpy), 8.72 (s, 1H, H3 of bpy), 8.58 (d, 1H, *J* = 4.8 Hz, H6' of bpy), 8.28 (s, 1H, H3' of bpy), 7.54 (d, 1H, *J* = 5.1 Hz, H5 of bpy), 7.23 (d, 1H, *J* = 4.5 Hz, H5' of bpy), 2.49 (s, 3H, CH<sub>3</sub> of bpy). MS (ESI, positive-ion mode): *m/z* 196 [M + H<sup>+</sup>]<sup>+</sup>.

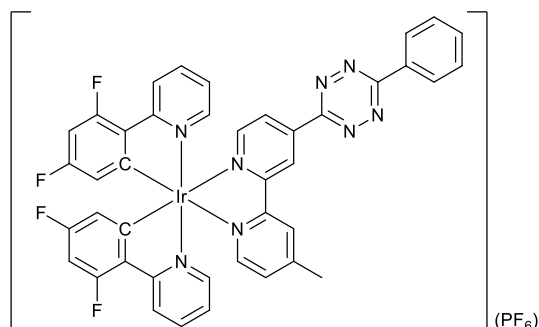


## bpy-Tz-Ph



To a mixture of bpy-CN (296 mg, 1.52 mmol), benzonitrile (0.79 mL, 7.60 mmol) and sulfur (49 mg, 1.52 mmol) in absolute EtOH (10 mL), hydrazine monohydrate (1.84 mL, 38 mmol) was added dropwise. The resulting mixture was refluxed at 70°C under an inert atmosphere of nitrogen for 18 h. The yellow precipitate was filtered and washed with cold EtOH (10 mL  $\times$  3). The precipitate was then added to sodium nitrite (1.05 g, 15.22 mmol) in 5 mL H<sub>2</sub>O, followed by the addition of 1 M HCl until pH = 3. The resulting mixture was neutralized by NH<sub>4</sub>OH solution and extracted with CH<sub>2</sub>Cl<sub>2</sub> (20 mL  $\times$  3). The combined organic extract was dried over MgSO<sub>4</sub> and evaporated to dryness under reduced pressure to give a purple solid, which was purified by column chromatography on silica gel. The desired product was eluted with CH<sub>2</sub>Cl<sub>2</sub>/MeOH (100:1, v/v). The solvent was removed under reduced pressure to afford the product as a purple solid. Yield: 112 mg (23%). <sup>1</sup>H NMR (300 MHz, CDCl<sub>3</sub>, 298 K):  $\delta$ 9.63 (s, 1H, H3 of bpy), 8.98 (d, 1H,  $J$  = 5.1 Hz, H6 of bpy), 8.74 – 8.71 (m, 2H, H2 and H6 of phenyl ring), 8.64 (d, 1H,  $J$  = 4.8 Hz, H6' of bpy), 8.51 – 8.49 (m, 1H, H5 of bpy), 8.33 (s, 1H, H3' of bpy), 7.73 – 7.63 (m, 3H, H3, H4 and H5 of phenyl ring), 7.22 (d, 1H,  $J$  = 4.8 Hz, H5' of bpy), 2.50 (s, 3H, CH<sub>3</sub> of bpy). MS (ESI, positive-ion mode):  $m/z$  327 [M + H]<sup>+</sup>.

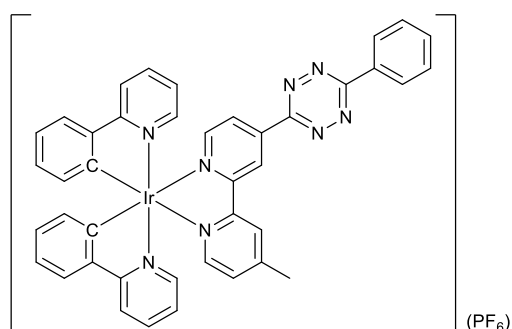
[Ir(dfppy)<sub>2</sub>(bpy-Tz-Ph)](PF<sub>6</sub>) (**1**)



A mixture of [Ir<sub>2</sub>(dfppy)<sub>4</sub>Cl<sub>2</sub>] (36 mg, 0.030 mmol) and bpy-Tz-Ph (21 mg, 0.065 mmol) in CH<sub>2</sub>Cl<sub>2</sub>/MeOH (20 mL, 1:1, v/v) was stirred under an inert atmosphere of nitrogen in the dark for 18 h. The mixture was further stirred for 2 h after addition of solid KPF<sub>6</sub> (27 mg, 0.15 mmol). The mixture was evaporated to dryness under reduced pressure to give an orange solid, which was purified by column chromatography on silica gel. The desired product was eluted with CH<sub>2</sub>Cl<sub>2</sub>/MeOH (50:1, v/v). The solvent was removed under reduced pressure to yield an orange solid. Subsequent recrystallization of the solid from CH<sub>2</sub>Cl<sub>2</sub>/Et<sub>2</sub>O afforded the complex as orange crystals. Yield: 30 mg (49%). <sup>1</sup>H NMR (300 MHz, CD<sub>3</sub>COCD<sub>3</sub>, 298 K): δ 9.79 (s, 1H, H3 of bpy-Tz-Ph), 9.24 (s, 1H, H3' of bpy-Tz-Ph), 8.79 (d, 1H, *J* = 5.7 Hz, H6 of bpy-Tz-Ph), 8.72 – 8.69 (m, 2H, H2 and H6 of phenyl ring of bpy-Tz-Ph), 8.57 (d, 1H, *J* = 5.7 Hz, H5 of bpy-Tz-Ph), 8.44 (d, 2H, *J* = 8.4 Hz, H6 of pyridyl ring of dfppy), 8.14 – 8.07 (m, 4H, H3 and H5 of pyridyl ring of dfppy), 8.02 (d, 1H, *J* = 6.6 Hz, H6' of bpy-Tz-Ph), 7.84 – 7.73 (m, 3H, H3, H4 and H5 of phenyl ring of bpy-Tz-Ph), 7.68 (d, 1H, *J* = 5.4 Hz, H5' of bpy-Tz-Ph), 7.31 – 7.25 (m, 2H, H4 of pyridyl ring of dfppy), 6.86 – 6.76 (m, 2H, H6 of phenyl ring of dfppy), 5.89 – 5.81 (m, 2H, H4 of phenyl ring of dfppy), 2.72 (s, 3H, CH<sub>3</sub> of bpy-Tz-Ph). <sup>13</sup>C NMR (150 MHz, CD<sub>3</sub>COCD<sub>3</sub>, 298 K): δ 166.5, 165.7, 165.6, 163.8, 162.4, 159.4, 156.7, 156.2, 156.1, 155.0, 154.2, 152.2, 151.8, 151.6, 145.0, 141.7, 135.4, 133.5, 131.9, 131.5, 130.1, 129.7, 128.5, 127.8, 126.02, 125.99,

125.61, 125.47, 123.9, 115.7, 115.6, 115.5, 100.88, 100.71, 100.64, 100.53, 100.46, 80.1, 55.9, 22.3. IR (KBr)  $\tilde{\nu}/\text{cm}^{-1}$ : 840 ( $\text{PF}_6^-$ ). MS (ESI, positive-ion mode):  $m/z$  899  $[\text{M} - \text{PF}_6^-]^+$ . Elemental analysis calculated (%) for  $\text{IrC}_{41}\text{H}_{26}\text{N}_8\text{PF}_6 \cdot \text{CH}_2\text{Cl}_2 \cdot \text{CH}_3\text{COCH}_3$ : C, 45.54; H, 2.89; N, 9.44; found: C, 45.73; H, 2.939; N, 9.24.

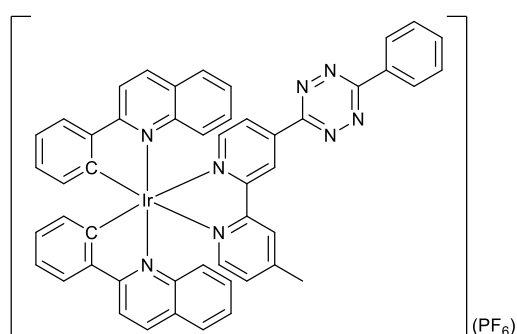
$[\text{Ir}(\text{ppy})_2(\text{bpy-Tz-Ph})](\text{PF}_6)$  (**2**)



The synthetic procedure was similar to that for **1**, except that  $[\text{Ir}_2(\text{ppy})_4\text{Cl}_2]$  (26 mg, 0.024 mmol) was used instead of  $[\text{Ir}_2(\text{dfppy})_4\text{Cl}_2]$ . Subsequent recrystallization of the solid from  $\text{CH}_2\text{Cl}_2/\text{Et}_2\text{O}$  afforded **2** as red crystals. Yield: 25 mg (53%).  $^1\text{H}$  NMR (300 MHz,  $\text{CD}_3\text{COCD}_3$ , 298 K):  $\delta$  9.75 (s, 1H, H3 of bpy-Tz-Ph), 9.15 (s, 1H, H3' of bpy-Tz-Ph), 8.74 – 8.68 (m, 3H, H2 and H6 of phenyl ring and H6 of bpy-Tz-Ph), 8.43 (d, 1H,  $J = 6.0$  Hz, H5 of bpy-Tz-Ph), 8.27 (d, 2H,  $J = 8.1$  Hz, H3 of pyridyl ring of ppy), 8.04 – 7.92 (m, 7H, H4 and H6 of pyridyl ring and H3 of phenyl ring of ppy and H6' of bpy-Tz-Ph), 7.82 – 7.71 (m, 3H, H3, H4 and H5 of phenyl ring of bpy-Tz-Ph), 7.62 (d, 1H,  $J = 5.7$  Hz, H5' of bpy-Tz-Ph), 7.22 – 7.16 (m, 2H, H5 of pyridyl ring of ppy), 7.10 – 7.03 (m, 2H, H4 of phenyl ring of ppy), 6.99 – 6.92 (m, 2H, H5 of phenyl ring of ppy), 6.44 – 6.37 (m, 2H, H6 of phenyl ring of ppy), 2.69 (s, 3H,  $\text{CH}_3$  of bpy-Tz-Ph).  $^{13}\text{C}$  NMR (150 MHz,  $\text{CD}_3\text{COCD}_3$ , 298 K):  $\delta$  169.6, 169.5, 169.4, 163.9, 159.6, 157.0, 154.3, 153.8, 152.1, 152.0, 151.8, 151.2, 151.1, 145.9, 145.8, 144.4, 140.55, 140.52, 135.3, 133.51, 133.50, 133.36,

132.3, 132.2, 131.5, 131.4, 130.1, 128.1, 127.5, 126.82, 126.75, 125.45, 125.43, 124.43, 124.38, 123.6, 121.79, 121.76, 55.9, 22.2. IR (KBr)  $\tilde{\nu}/\text{cm}^{-1}$ : 840 ( $\text{PF}_6^-$ ). MS (ESI, positive-ion mode):  $m/z$  827 [ $\text{M} - \text{PF}_6^-$ ] $^+$ . Elemental analysis calculated (%) for  $\text{IrC}_{41}\text{H}_{30}\text{N}_8\text{PF}_6 \cdot \text{CH}_3\text{COCH}_3$ : C, 51.35; H, 3.52; N, 10.88; found: C, 51.47; H, 3.429; N, 10.65.

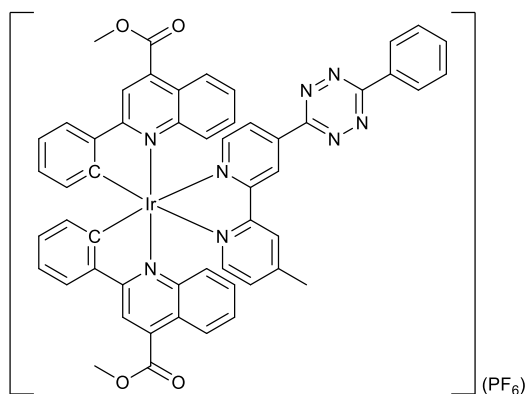
$[\text{Ir}(\text{pq})_2(\text{bpy-Tz-Ph})](\text{PF}_6)$  (**3**)



The synthetic procedure was similar to that for **1**, except that  $[\text{Ir}_2(\text{pq})_4\text{Cl}_2]$  (37 mg, 0.029 mmol) was used instead of  $[\text{Ir}_2(\text{dfppy})_4\text{Cl}_2]$ . Subsequent recrystallization of the solid from  $\text{CH}_2\text{Cl}_2/\text{Et}_2\text{O}$  afforded **3** as dark red crystals. Yield: 39 mg (63%).  $^1\text{H}$  NMR (300 MHz,  $\text{CD}_3\text{COCD}_3$ , 298 K):  $\delta$  9.35 (s, 1H, H3 of bpy-Tz-Ph), 8.72 – 8.69 (m, 3H, H3', H5 and H6 of bpy-Tz-Ph), 8.62 (d, 2H,  $J = 6.9$  Hz, H2 and H6 of phenyl ring of bpy-Tz-Ph), 8.57 – 8.50 (m, 4H, H3 and H4 of quinoline of pq), 8.30 – 8.25 (m, 3H, H3 of phenyl ring of pq and H6' of bpy-Tz-Ph), 7.96 – 7.89 (m, 2H, H8 of quinoline of pq), 7.77 – 7.67 (m, 3H, H3, H4 and H5 of phenyl ring of bpy-Tz-Ph), 7.62 – 7.48 (m, 3H, H5 of quinoline of pq and H5' of bpy-Tz-Ph), 7.43 (t, 2H,  $J = 7.4$  Hz, H7 of quinoline of pq), 7.22 – 7.14 (m, 4H, H6 of quinoline and H4 of phenyl ring of pq), 6.87 – 6.79 (m, 2H, H5 of phenyl ring of pq), 6.66 – 6.59 (m, 2H, H6 of phenyl ring of pq), 2.53 (s, 3H,  $\text{CH}_3$  of bpy-Tz-Ph).  $^{13}\text{C}$  NMR (150 MHz,  $\text{CD}_3\text{COCD}_3$ , 298 K):  $\delta$  172.2, 172.1, 166.3, 163.6, 159.1, 156.6, 154.3, 152.7, 152.6, 151.3, 149.30, 149.27, 149.24, 147.9, 147.8, 144.5, 142.24, 142.22, 136.2, 136.1,

135.3, 133.5, 132.95, 132.88, 132.51, 132.47, 131.40, 131.28, 131.23, 131.15, 130.1, 129.8, 129.4, 129.2, 128.6, 127.4, 127.1, 126.64, 126.60, 124.84, 124.82, 122.70, 120.0, 119.9, 55.9, 22.0. IR (KBr)  $\tilde{\nu}/\text{cm}^{-1}$ : 842 ( $\text{PF}_6^-$ ). MS (ESI, positive-ion mode):  $m/z$  927  $[\text{M} - \text{PF}_6^-]^+$ . Elemental analysis calculated (%) for  $\text{IrC}_{49}\text{H}_{34}\text{N}_8\text{PF}_6 \cdot \text{CH}_3\text{COCH}_3$ : C, 55.27; H, 3.57; N, 9.92; found: C, 54.98; H, 3.50; N, 9.73.

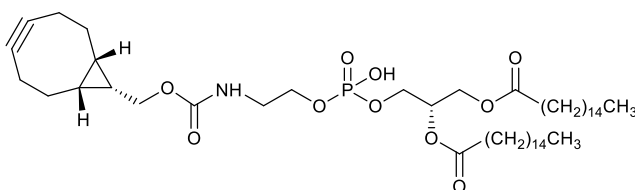
**[Ir(pqe)<sub>2</sub>(bpy-Tz-Ph)](PF<sub>6</sub>) (**4**)**



The synthetic procedure was similar to that for **1**, except that  $[\text{Ir}_2(\text{pqe})_4\text{Cl}_2]$  (35 mg, 0.023 mmol) was used instead of  $[\text{Ir}_2(\text{dfppy})_4\text{Cl}_2]$ . Subsequent recrystallization of the solid from  $\text{CH}_2\text{Cl}_2/\text{Et}_2\text{O}$  afforded **4** as red crystals. Yield: 25 mg (46%).  $^1\text{H}$  NMR (300 MHz,  $\text{CD}_3\text{COCD}_3$ , 298 K):  $\delta$  9.39 (s, 1H, H3 of bpy-Tz-Ph), 8.93 (d, 2H,  $J = 3.3$  Hz, H3 of quinoline of pqe), 8.83 (s, 1H, H3' of bpy-Tz-Ph), 8.77 – 8.75 (m, 1H, H6 of bpy-Tz-Ph), 8.71 (d, 1H,  $J = 6.0$  Hz, H5 of bpy-Tz-Ph), 8.65 (d, 2H,  $J = 6.9$  Hz, H2 and H6 of phenyl ring of bpy-Tz-Ph), 8.55 – 8.49 (m, 2H, H5 of quinoline of pqe), 8.41 – 8.37 (m, 2H, H3 of phenyl ring of pqe), 8.27 (d, 1H,  $J = 5.4$  Hz, H6' of bpy-Tz-Ph), 7.81 – 7.64 (m, 6H, H8 of quinoline of pqe and H3, H4 and H5 of phenyl ring and H5' of bpy-Tz-Ph), 7.54 (t, 2H,  $J = 7.7$  Hz, H7 of quinoline of pqe), 7.30 – 7.21 (m, 4H, H6 of quinoline and H4 of phenyl ring of pqe), 6.96 – 6.89 (m, 2H, H5 of phenyl ring of pqe), 6.71 –

6.65 (m, 2H, H6 of phenyl ring of ppe), 4.15 (s, 3H, COOCH<sub>3</sub>), 4.11 (s, 3H, COOCH<sub>3</sub>), 2.57 (s, 3H, CH<sub>3</sub> of bpy-Tz-Ph). <sup>13</sup>C NMR (150 MHz, CD<sub>3</sub>COCD<sub>3</sub>, 298 K): δ 172.0, 171.9, 167.1, 166.3, 163.6, 158.9, 156.3, 154.7, 152.8, 152.7, 151.3, 149.9, 149.3, 147.4, 147.3, 144.7, 141.0, 140.9, 136.5, 136.4, 135.3, 133.46, 133.12, 133.10, 133.06, 131.6, 131.4, 130.1, 129.9, 129.8, 129.7, 128.6, 128.5, 127.53, 127.35, 127.22, 127.19, 126.2, 125.2, 122.8, 120.9, 120.7, 55.9, 54.62, 54.59, 22.0. IR (KBr)  $\tilde{\nu}/\text{cm}^{-1}$ : 1726 (C=O), 841 (PF<sub>6</sub><sup>-</sup>). MS (ESI, positive-ion mode): *m/z* 1043 [M – PF<sub>6</sub><sup>-</sup>]<sup>+</sup>. Elemental analysis calculated (%) for IrC<sub>49</sub>H<sub>34</sub>N<sub>8</sub>PF<sub>6</sub>·CH<sub>3</sub>OH: C, 53.16; H, 3.47; N, 9.18; found: C, 52.99; H, 3.29; N, 8.92.

*N*-[(1*R*,8*S*,9*S*)-Bicyclo[6.1.0]non-4-yn-9-ylmethoxycarbonyl]-1,2-dipalmitoyl-*sn*-glycero-3-phosphoethanolamine (**BCN-DPPE**)



To a solution of 1,2-dipalmitoyl-*sn*-glycero-3-phosphoethanolamine (15 mg, 0.02 mmol) in CH<sub>2</sub>Cl<sub>2</sub> (3 mL) were added **BCN-NHS** (6.3 mg, 0.02 mmol) and Et<sub>3</sub>N (15 μL, 1.0 mmol). The mixture was stirred at room temperature under an inert atmosphere of N<sub>2</sub> in the dark for 18 h. The solvent was evaporated under reduced pressure and the crude product was purified by column chromatography on silica gel using CH<sub>2</sub>Cl<sub>2</sub>/MeOH (20:1, v/v) as the eluent. The solvent was removed under reduced pressure and the product was subsequently isolated as a white solid. Yield: 14.1 mg (75%). <sup>1</sup>H NMR (300 MHz, CDCl<sub>3</sub>, 298 K): δ 5.27 – 5.23 (m, 1H, CH), 4.35 – 4.16 (m, 8H, BCN, NCH<sub>2</sub>CH<sub>2</sub>O and CHCH<sub>2</sub>O), 3.89 (br, 1H, OCONH), 3.50 – 3.46 (m, 2H, NCH<sub>2</sub>CH<sub>2</sub>O), 3.16 – 3.14 (m, 6H, Et<sub>3</sub>N), 2.74 – 2.72 (m, 2H, OCOCH<sub>2</sub>), 2.35 – 2.26 (m, 6H, BCN

and  $\text{OCOCH}_2$ ), 1.64 – 1.58 (m, 5H, BCN), 1.30 – 1.24 (m, 52H,  $\text{CH}_2$ ), 0.91 – 0.84 (m, 17H, BCN,  $\text{Et}_3\text{N}$  and  $\text{CH}_3$ ).  $^{13}\text{C}$  NMR (75 MHz,  $\text{CDCl}_3$ , 298 K, TMS): 172.6, 130.9, 128.8, 99.0, 68.2, 45.7, 38.7, 34.1, 32.0, 30.4, 29.7, 29.6, 29.4, 29.2, 28.9, 25.5, 24.9, 23.7, 23.0, 22.7, 21.5, 14.2, 14.1, 11.0, 8.6. MS (ESI, positive-ion mode):  $m/z$  969  $[\text{M} + \text{Et}_3\text{N} + \text{H}^+]^+$ .

### Preparation of Pyridazine and Dihydropyridazine Derivatives

To the iridium(III) complexes (20  $\mu\text{mol}$ ) or bpy-Tz-Ph (20  $\mu\text{mol}$ ) in 800  $\mu\text{L}$   $\text{CH}_2\text{Cl}_2$ , **BCN-OH** (40  $\mu\text{mol}$ ) or **TCO-OH** (40  $\mu\text{mol}$ ) in  $\text{CH}_2\text{Cl}_2/\text{MeOH}$  (200  $\mu\text{L}$ , 1:1, v/v) was added and stirred under an inert atmosphere of  $\text{N}_2$  at room temperature in the dark for 18 h. The crude product was purified by column chromatography on silica gel using  $\text{CH}_2\text{Cl}_2/\text{MeOH}$  as the eluent. The solution was rotary evaporated to dryness to give yellow to orange solids, which were washed with  $\text{Et}_2\text{O}$  and dried in vacuo. The formation of the pyridazine and dihydropyridazine derivatives were confirmed by ESI-MS analysis.

### Determination of Lipophilicity

The lipophilicity ( $\log P_{o/w}$ ) of the complexes was measured using the shake-flask method.<sup>9</sup> An aliquot of stock solution of the complex in octan-1-ol (saturated with 0.9% NaCl, w/v) was added to an equal volume of aqueous NaCl solution (0.9% w/v and saturated with octan-1-ol). The mixture was shaken at 60 rpm for 2 h to allow partitioning at 298 K. The solution was then centrifuged and the amounts of complex in organic layer ( $[\text{Ir}]_o$ ) was determined by emission spectroscopy. The partition coefficient ( $P_{o/w}$ ) for each complex was calculated as the ratio of  $[\text{Ir}]_o/[\text{Ir}]_w$ , where  $[\text{Ir}]_w$  was obtained by subtraction of the total amount of complex by the amount in the organic phase after partitioning.

### Solubility Tests

The solubility of complexes **1** – **4** was determined by electronic absorption spectroscopy. Complexes of different concentrations in solvents including  $\text{CH}_2\text{Cl}_2$ ,  $\text{CH}_3\text{CN}$  and potassium



phosphate buffer (50 mM, pH 7.4)/DMSO (99:1, v/v), together with their saturated solutions were prepared and the absorbance was measured. Linear plots of absorbance versus concentrations were constructed. The concentrations of the complexes in the saturated solutions were then determined.

### Photostability and Photobleaching Studies

For photostability studies, the iridium(III) complexes (10  $\mu$ M) in 2 mL potassium phosphate buffer (50 mM, pH 7.4)/DMSO (99:1, v/v) was introduced into a quartz cuvette of 1 cm path length and irradiated with 365 nm (1 mW/cm<sup>2</sup>). The absorbance of the solutions at *ca.* 310 nm were monitored every 60 s. The procedures for photobleaching studies were similar except that the emission of the solutions at their emission maxima was examined instead of absorbance.

### Förster Distance Measurements

The Förster distance ( $R_0$ ) was calculated according to the following equation:

$$R_0(\text{in } \text{Å}) = 0.211 \times \sqrt[6]{\kappa^2 \times n^{-4} \times \Phi_D \times J(\lambda)}$$

where  $\kappa^2$  is a factor describing the relative orientation in space of the transition dipoles of the donor (D) and the acceptor (A) and is assumed to be 2/3;  $n$  is the refractive index of the solvent;  $\Phi_D$  is the emission quantum yield of the iridium(III) complex without the tetrazine unit;  $J(\lambda)$  is the overlap integral of the donor emission and the acceptor absorption spectra. Calculation of  $J(\lambda)$  is based on the equation below:

$$J(\lambda) = \int_0^{\infty} F_D(\lambda) \times \varepsilon_A(\lambda) \times \lambda^4 d\lambda$$

where  $F_D$  is the corrected emission intensity of the donor with the emission intensity normalized to unity and  $\varepsilon_A$  is the absorption coefficient of the acceptor.

Calculated energy transfer efficiency ( $E_{\text{calc}}$ ) based on Förster's theory was determined according to the following equation:

$$E_{\text{calc}} = \frac{R_0^6}{R_0^6 + r^6}$$

where  $r$  is the distance between the iridium(III) metal centre and the tetrazine unit, which was estimated by the three-dimensional structures of the iridium(III) complexes modulated by Chem3D 16.0.

### Kinetics Studies

The reaction kinetics of the free ligand bpy-Tz-Ph (5  $\mu\text{M}$ ) and the complexes (5  $\mu\text{M}$ ) with **BCN-OH** (50 – 300  $\mu\text{M}$ ) or **TCO-OH** (30 – 80  $\mu\text{M}$ ) in MeOH/H<sub>2</sub>O (1:1, v/v) at 298 K were measured by electronic absorption spectroscopy. The reactions were monitored by following the exponential decay of the absorbance at ca. 306 nm upon addition of **BCN-OH** or **TCO-OH**. Data were fitted to a single-exponential equation to give the pseudo first order rate constants  $k_{\text{obs}}$ , which were then plotted against the concentrations of **BCN-OH** or **TCO-OH** to obtain the second order rate constants  $k_2$  as the slopes of the plots.

## Determination of Singlet Oxygen Generation Quantum Yields ( $\Phi_{\Delta}$ )

An air-equilibrated CH<sub>3</sub>CN solution (2 mL) containing the iridium(III) complexes and DPBF (50  $\mu$ M) was introduced into a quartz cuvette of 1 cm path length and irradiated with the 365 or 450 nm output of a HORIBA Jobin Yvon FluoroMax-4 spectrofluorometer as an excitation source. Phenalenone was used as a reference for <sup>1</sup>O<sub>2</sub> sensitisation ( $\Phi_{\Delta} = 0.97$ )<sup>10</sup> at 365 nm and [Ru(bpy)<sub>3</sub>]Cl<sub>2</sub> ( $\Phi_{\Delta} = 0.57$ )<sup>11</sup> was used at 450 nm. The absorbance of the complexes and references at 365 or 450 nm was *ca.* 0.15. The absorbance of DPBF at 410 nm was monitored every 10 s. A CH<sub>3</sub>CN solution of DPBF without the complexes was examined to determine its photostability under identical irradiation conditions. The  $\Phi_{\Delta}$  of the complex was determined by comparing  $\Phi_{\Delta}$  of iridium(III)-sensitized DPBF photooxidation to  $\Phi_{\Delta}$  of phenalenone-sensitized DPBF photooxidation (as reference) and calculated by the following equation:

$$\Phi_{\Delta}^{unknown} = \Phi_{\Delta}^{reference} \times \frac{m^{unknown} \times F^{reference}}{m^{reference} \times F^{unknown}}$$

where  $m$  is the slope of a linear fit of the change in absorbance of DPBF at 410 nm against the irradiation time and  $F$  is the absorption correlation factor, which is given as  $F = 1 - 10^{-AL}$  ( $A$  = absorbance at 365 or 450 nm and  $L$  = pathlength of the cuvette).

## Protein Labelling Studies

*Modification of BSA with BCN-NHS or TCO-NHS.* BCN-NHS or TCO-NHS (1.00 mg, 3.43  $\mu$ mol) in 100  $\mu$ L anhydrous DMSO was added to BSA (23 mg, 0.35  $\mu$ mol) in 400  $\mu$ L carbonate buffer (50 mM, pH 10). The mixture was incubated in the dark at 298 K for 24 h. The solution was loaded onto a PD-10 size exclusion column that had been pre-equilibrated with potassium phosphate buffer (50 mM, pH 7.4). Volume fractions between 2.5 and 5.0 mL were collected

and washed with the same buffer with a YM-10 microcon filter. The volume of the modified BSA was reduced to 1.0 mL and its concentration was determined by a NanoDrop 1000 spectrophotometer. The protein was stored at  $-20^{\circ}\text{C}$  before use.

*Labelling of **BCN-BSA** or **TCO-BSA** with the complexes.* The complex (1 nmol) in anhydrous DMSO (1  $\mu\text{L}$ ) was added to the **BCN-BSA** or **TCO-BSA** (0.25 nmol) in potassium phosphate buffer (50 mM, pH 7.4) (99  $\mu\text{L}$ ). The mixture was stirred in the dark at 298 K for 18 h. An aliquot (10  $\mu\text{L}$ ) of the reaction mixture was analysed by SDS-PAGE to confirm the conjugation of the complexes to **BCN-BSA** or **TCO-BSA**.

### **Live-cell Co-staining Experiments of BCN Derivatives**

HeLa cells in growth medium were seeded on a sterilized coverslip in a 35-mm tissue culture dish and grown at  $37^{\circ}\text{C}$  under a 5%  $\text{CO}_2$  atmosphere for 48 h. The growth medium was replaced with either fresh medium or **BCN-morph** (50  $\mu\text{M}$ ) or **BCN-DPPE** (50  $\mu\text{M}$ ) in medium/DMSO (99:1, v/v) for 2 h. The cells were thoroughly washed with PBS (1 mL  $\times$  3) and further incubated with complex **2** (10  $\mu\text{M}$ ) in medium/DMSO (99:1, v/v) for 2 h. The cells were then washed with PBS (1 mL  $\times$  3) and incubated with LysoTracker Deep Red (100 nM) for 1 h or ER-Tracker Green (1  $\mu\text{M}$ ) in growth medium for 20 min. The medium was removed and the cell layer was gently washed with PBS (1 mL  $\times$  3). The coverslip was mounted onto a sterilized glass slide and imaging was performed using a Leica TCS SPE (inverted configuration) confocal microscope with an oil immersion 63x objective. The excitation wavelength of the complex, LysoTracker Deep Red and ER-Tracker Green were 405, 635 and 488 nm, respectively. The

Pearson's correlation coefficients were determined using the program ImageJ (Version 1.4.3.67).

### **Preparation of Lipoplexes**

Lipoplexes were prepared according to the instruction of the manufacturer with a ratio of Lipofectamine 3000:plasmid (2  $\mu$ L:1  $\mu$ g). In brief, Lipofectamine 3000 reagent (4  $\mu$ L) was diluted to 100  $\mu$ L with Opti-MEM. The pHTN HaloTag CMV-neo Vector (2  $\mu$ g) in Opti-MEM (96  $\mu$ L), which is the DNA plasmid encoding the HaloTag protein, was gently mixed with P3000 reagent (4  $\mu$ L). The two solutions were then combined, mixed gently and incubated for an additional 15 min to allow the formation of lipoplexes.

### **Live-cell Confocal Imaging of HaloTag**

HeLa cells in growth medium were seeded on a sterilized coverslip in a 35-mm tissue culture dish and grown at 37°C under a 5% CO<sub>2</sub> atmosphere for 48 h. The cells were transfected by adding 100  $\mu$ L lipoplexes of pHTN HaloTag CMV-neo Vector to each well and incubated for 18 h prior to imaging studies. The growth medium was then removed and replaced with **BCN-C6-Cl** (50  $\mu$ M) or **TCO-C6-Cl** (50  $\mu$ M) in medium/DMSO (99:1, v/v) for 1 h. The cells were washed with PBS (1 mL  $\times$  3) and further incubated in fresh medium (2 mL) for 1 h. The medium was then replaced with the iridium(III) complexes (10  $\mu$ M) in medium/DMSO (99:1, v/v). After incubation for 1 h, the coverslip was mounted onto a sterilized glass slide and imaging was performed using a Leica TCS SPE (inverted configuration) confocal microscope with an oil

immersion 63x objective and an excitation wavelength at 405 nm. Control experiments of cells without transfection and treatment of **BCN-C6-Cl** and **TCO-C6-Cl** were also carried out.

### MTT Assays

HeLa cells were seeded in two 96-well flat-bottomed microplates (*ca.* 10,000 cells/well) in growth medium (100  $\mu$ L) and grown at 37°C under a 5% CO<sub>2</sub> atmosphere for 24 h. The cells were transfected by adding 10  $\mu$ L lipoplexes of pHTN HaloTag CMV-neo Vector to each well. Cells were pretreated with **BCN-C6-Cl** (50  $\mu$ M) or **TCO-C6-Cl** (50  $\mu$ M) in medium/DMSO (99:1, *v/v*) for 1 h. The complexes were then added to the wells with concentrations ranging from 10<sup>-7</sup> to 10<sup>-4</sup> M in medium/DMSO (99:1, *v/v*) and the cells were incubated at 37°C under a 5% CO<sub>2</sub> atmosphere for 1 h. Wells containing untreated cells were used as blank control. After the treatment, the culture medium was replaced with phenol red-free medium. One of the microplates was irradiated at 365 nm (5 mW/cm<sup>2</sup>) for 5 min in a LED cellular photocytotoxicity irradiators (PURI Materials, ShenZhen, China) and the other microplate was kept in the dark. The culture medium was then replaced with fresh medium and the cells were incubated at 37°C under a 5% CO<sub>2</sub> atmosphere. After incubation for 20 h, the medium in each well was replaced with fresh medium (90  $\mu$ L) and 10  $\mu$ L of MTT (5 mg/mL) in PBS was added. The medium was removed after incubation at 37°C for 3 h and DMSO (200  $\mu$ L) was added to each well. The absorbance of the solutions at 570 nm was measured with a BioTek Powerwave XS MQX200R microplate spectrophotometer. The IC<sub>50</sub> values of the complexes were determined from dose dependence of surviving cells after exposure to the complexes.

### **Inductively Coupled Plasma-Mass Spectroscopy (ICP-MS)**

HeLa cells were grown in a 60-mm tissue culture dish and incubated at 37°C under a 5% CO<sub>2</sub> atmosphere for 48 h. Cells were first transfected with 200 µL lipoplexes and incubated with a mixture of medium/DMSO (99:1, v/v) containing **BCN-C6-Cl** (50 µM) or **TCO-C6-Cl** (50 µM) for 1 h. The cells were washed with PBS (1 mL × 3) and further incubated in fresh medium (2 mL) for 1 h. After the medium was removed, the cells were washed thoroughly with PBS (1 mL × 3) and incubated with the complexes (10 µM) in medium/DMSO (99:1, v/v) for 1 h. After 1 h, the cells were washed with PBS (1 mL × 3) and then further incubated in fresh medium (5 mL) for another 1 h. The cells were then trypsinized and harvested with PBS. The resultant solution (1 mL) was digested with 65% HNO<sub>3</sub> (1 mL) at 60°C for 2 h and cooled to room temperature. The concentration of iridium was measured using a Perkin Elmer PE NexION 2000 ICP-MS.

**Table S1** Electronic absorption spectral data of complexes **1** – **4** and bpy-Tz-Ph in CH<sub>2</sub>Cl<sub>2</sub> and CH<sub>3</sub>CN at 298 K.

Compound	Solvent	$\lambda_{\text{abs}}/\text{nm}$ ( $\epsilon/\text{dm}^3 \text{ mol}^{-1} \text{ cm}^{-1}$ )
<b>1</b>	CH <sub>2</sub> Cl <sub>2</sub>	265 sh (45,270), 314 (46,330), 366 sh (19,760), 388 sh (12,595), 482 (2,010)
	CH <sub>3</sub> CN	265 sh (43,495), 302 (46,210), 359 sh (17,445), 381 sh (9,320), 447 (1,705)
<b>2</b>	CH <sub>2</sub> Cl <sub>2</sub>	255 (47,300), 271 (43,745), 311 (44,120), 380 (14,325), 403 sh (11,815), 535 (1,705)
	CH <sub>3</sub> CN	254 (45,700), 268 (44,015), 302 (44,410), 367 (13,435), 389 sh (11,655), 503 (1,485)
<b>3</b>	CH <sub>2</sub> Cl <sub>2</sub>	262 sh (47,575), 283 (54,350), 321 (44,085), 353 sh (26,630), 431 (7,960), 532 (1,765)
	CH <sub>3</sub> CN	261 sh (45,915), 282 (53,415), 312 (39,915), 349 sh (23,400), 425 (6,000), 518 (1,270)
<b>4</b>	CH <sub>2</sub> Cl <sub>2</sub>	265 (52,405), 294 (61,380), 323 (46,325), 370 sh (32,245), 417 sh (10,675), 476 (5,670)
	CH <sub>3</sub> CN	266 (49,220), 291 (62,825), 320 (41,975), 366 sh (28,630), 418 sh (7,170), 466 (4,845)
bpy-Tz-Ph	CH <sub>2</sub> Cl <sub>2</sub>	255 (16,435), 292 (39,775), 550 (430)
	CH <sub>3</sub> CN	254 (16,135), 291 (38,760), 539 (425)



**Table S2** Photophysical data of complexes **1** – **4**.

Complex	Medium (T/K)	$\lambda_{em}/nm$	$\Phi_{em}$	$\tau_0/\mu s$
<b>1</b>	CH <sub>2</sub> Cl <sub>2</sub> (298)	551	0.0142	1.03
	CH <sub>3</sub> CN (298)	557	0.0074	0.61
	Buffer (298) <sup>a</sup>	556	0.0049	0.49
	Glass (77) <sup>b</sup>	486 (max), 528, 565 sh		
<b>2</b>	CH <sub>2</sub> Cl <sub>2</sub> (298)	594	0.0044	0.41
	CH <sub>3</sub> CN (298)	606	0.0017	0.18
	Buffer (298) <sup>a</sup>	601	0.0008	0.16
	Glass (77) <sup>b</sup>	548, 589 sh		
<b>3</b>	CH <sub>2</sub> Cl <sub>2</sub> (298)	558, 599 sh	0.0111	1.16
	CH <sub>3</sub> CN (298)	561, 596 sh	0.0077	1.06
	Buffer (298) <sup>a</sup>	561, 596 sh	0.0062	0.98
	Glass (77) <sup>b</sup>	543 (max), 584, 638 sh		
<b>4</b>	CH <sub>2</sub> Cl <sub>2</sub> (298)	619	0.0202	1.33
	CH <sub>3</sub> CN (298)	637	0.0033	0.24
	Buffer (298) <sup>a</sup>	647	0.0013	0.15
	Glass (77) <sup>b</sup>	593, 643 sh		

<sup>a</sup> PBS (1X, pH 7.4)/CH<sub>3</sub>CN (1:1, v/v). <sup>b</sup> EtOH/MeOH (4:1, v/v).

**Table S3** Lipophilicity ( $\log P_{o/w}$ ) and solubility of complexes **1** – **4** at 298 K.

Complexes	$\log P_{o/w}^a$		Solubility (mM)	
<b>1</b>	1.16	7.2 <sup>b</sup>	6.6 <sup>c</sup>	0.11 <sup>d</sup>
<b>2</b>	0.66	> 50.0 <sup>b</sup>	25.4 <sup>c</sup>	0.12 <sup>d</sup>
<b>3</b>	1.34	> 50.0 <sup>b</sup>	> 50.0 <sup>c</sup>	0.065 <sup>d</sup>
<b>4</b>	1.18	> 50.0 <sup>b</sup>	24.1 <sup>c</sup>	0.094 <sup>d</sup>

<sup>a</sup>  $\log P_{o/w}$  is defined as the logarithmic ratio of the concentration of the iridium complex in saturated octan-1-ol with NaCl to that in an aqueous solution of NaCl (0.9%, w/v). <sup>b</sup> Measured in aerated CH<sub>2</sub>Cl<sub>2</sub>. <sup>c</sup> Measured in aerated CH<sub>3</sub>CN. <sup>d</sup> Measured in aerated potassium phosphate buffer (50 mM, pH 7.4)/DMSO (99:1, v/v).

**Table S4** FRET parameters of complexes **1 – 4**.

Complex	Donor	Acceptor	$J(\lambda)^a/\text{nm}^4 \text{M}^{-1} \text{cm}^{-1}$	$R_0/\text{\AA}$	$d^b/\text{\AA}$	$E_{\text{calc}}$
<b>1</b>	[Ir(dfppy) <sub>2</sub> (bpy)](PF <sub>6</sub> )	bpy-Tz-Ph	$1.95 \times 10^{13}$	26.39	6.95	0.99
<b>2</b>	[Ir(pppy) <sub>2</sub> (bpy)](PF <sub>6</sub> )	bpy-Tz-Ph	$1.40 \times 10^{13}$	19.68	7.33	0.99
<b>3</b>	[Ir(pq) <sub>2</sub> (bpy)](PF <sub>6</sub> )	bpy-Tz-Ph	$1.67 \times 10^{13}$	24.56	5.91	0.99
<b>4</b>	[Ir(pqe) <sub>2</sub> (bpy)](PF <sub>6</sub> )	bpy-Tz-Ph	$4.68 \times 10^{11}$	7.43	5.95	0.79

<sup>a</sup> Overlap integral of the emission spectrum of the iridium(III) complex (donor) and the absorption spectrum of bpy-Tz-Ph (acceptor). <sup>b</sup> Distance between the iridium(III) atom and tetrazine moiety in complexes **1 – 4**.

**Table S5** Electrochemical data of complexes **1** – **4** and bpy-Tz-Ph.<sup>a</sup>

Compound	Oxidation, $E_{1/2}/V$	Reduction, $E_{1/2}$ or $E_c/V$
<b>1</b>	+1.61 <sup>b</sup>	-0.65, -1.37, <sup>b</sup> -1.82, <sup>c</sup> -2.04, <sup>c</sup> -2.30 <sup>c</sup>
<b>2</b>	+1.29 <sup>b</sup>	-0.67, -1.44, <sup>b</sup> -1.80, <sup>c</sup> -2.17, <sup>c</sup> -2.45 <sup>c</sup>
<b>3</b>	+1.31 <sup>b</sup>	-0.66, -1.45, <sup>b</sup> -1.73, <sup>c</sup> -1.95, <sup>c</sup> -2.19 <sup>c</sup>
<b>4</b>	+1.39 <sup>b</sup>	-0.66, <sup>b</sup> -1.08, <sup>b</sup> -1.24, <sup>b</sup> -1.61, <sup>c</sup> -1.91, <sup>c</sup> -2.13 <sup>c</sup>
bpy-Tz-Ph	+1.78 <sup>b</sup>	-0.77, -1.74, <sup>b</sup> -1.97, <sup>c</sup> -2.22 <sup>c</sup>

<sup>a</sup> In CH<sub>3</sub>CN (0.1 mol dm<sup>-3</sup> TBAP) at 298 K, glassy carbon electrode, sweep rate = 100 mV s<sup>-1</sup>, all potential versus SCE. <sup>b</sup> Quasi-reversible couples. <sup>c</sup> Irreversible waves.

**Table S6** Electrochemical data of complexes **1b** – **4b** and bpy-TCO-Ph.<sup>a</sup>

Compound	Oxidation, $E_{1/2}$ or $E_a/V$	Reduction, $E_{1/2}$ or $E_c/V$
<b>1b</b>	+0.91, <sup>b</sup> +1.60 <sup>b</sup>	-1.31, -1.85, <sup>b</sup> -2.06 <sup>c</sup>
<b>2b</b>	+1.26 <sup>b</sup>	-1.33, -1.86, <sup>b</sup> -2.03 <sup>c</sup>
<b>3b</b>	+1.31 <sup>b</sup>	-1.34, -1.77, -1.96 <sup>b</sup>
<b>4b</b>	+1.35 <sup>b</sup>	-1.10, -1.27, -1.68, <sup>b</sup> -2.04 <sup>c</sup>
bpy-TCO-Ph	+0.90 <sup>b</sup>	-1.43, <sup>b</sup> -2.06, <sup>c</sup> -2.28 <sup>c</sup>

<sup>a</sup> In CH<sub>3</sub>CN (0.1 mol dm<sup>-3</sup> TBAP) at 298 K, glassy carbon electrode, sweep rate = 100 mV s<sup>-1</sup>, all potential versus SCE. <sup>b</sup> Quasi-reversible couples. <sup>c</sup> Irreversible waves.

**Table S7** Second-order rate constants ( $k_2$ ) of complexes **1** – **4** and bpy-Tz-Ph upon reactions with **BCN-OH** and **TCO-OH** in a mixture of MeOH/H<sub>2</sub>O (1:1, v/v) at 298 K.

Compound	$k_2/\text{M}^{-1} \text{s}^{-1}$	
	<b>BCN-OH</b>	<b>TCO-OH</b>
<b>1</b>	$23.8 \pm 0.6$	$676.8 \pm 18.5$
<b>2</b>	$20.9 \pm 0.4$	$634.6 \pm 7.4$
<b>3</b>	$74.2 \pm 2.0$	$1313.1 \pm 34.7$
<b>4</b>	$83.1 \pm 2.4$	$1471.3 \pm 39.6$
bpy-Tz-Ph	$29.1 \pm 0.9$	$188.0 \pm 5.6$

**Table S8**  $^1\text{O}_2$  generation quantum yields ( $\Phi_\Delta$ ) of complexes **1 – 4**, **1a – 4a** and **1b – 4b** in aerated  $\text{CH}_3\text{CN}$  at 298 K. DPBF was used as the  $^1\text{O}_2$  scavenger.

Complex	$\Phi_\Delta^a$	$\Phi_\Delta^b$
<b>1</b>	0.82	0.42
<b>1a</b>	0.76	0.32
<b>1b</b>	0.36	0.12
<b>2</b>	0.63	0.43
<b>2a</b>	0.46	0.31
<b>2b</b>	0.27	0.23
<b>3</b>	0.66	0.66
<b>3a</b>	0.31	0.47
<b>3b</b>	0.23	0.33
<b>4</b>	0.61	0.73
<b>4a</b>	0.56	0.65
<b>4b</b>	0.26	0.34

<sup>a</sup>  $\lambda_{\text{ex}} = 365$  nm and phenalenone was adopted as the reference. <sup>b</sup>  $\lambda_{\text{ex}} = 450$  nm and  $[\text{Ru}(\text{bpy})_3]\text{Cl}_2$  was adopted as the reference.

**Table S9** Cytotoxicity of complex **2** towards transfected HeLa cells in the dark and upon irradiation at 365 nm for 5 min. PI is the ratio of  $IC_{50, \text{dark}}/IC_{50, \text{light}}$  under different conditions.

Cells without treatment			Cells with <b>BCN-C6-Cl</b> <sup>a</sup>			Cells with <b>TCO-C6-Cl</b> <sup>b</sup>		
$IC_{50, \text{dark}}/\mu\text{M}$	$IC_{50, \text{light}}/\mu\text{M}$	<b>PI</b>	$IC_{50, \text{dark}}/\mu\text{M}$	$IC_{50, \text{light}}/\mu\text{M}$	<b>PI</b>	$IC_{50, \text{dark}}/\mu\text{M}$	$IC_{50, \text{light}}/\mu\text{M}$	<b>PI</b>
> 50	0.68 ± 0.05	> <b>74.1</b>	> 50	0.26 ± 0.09	> <b>196.1</b>	> 50	1.00 ± 0.09	> <b>50.0</b>

<sup>a</sup> Pretreatment of **BCN-C6-Cl** (50  $\mu\text{M}$ ) for 1 h, followed by washing with PBS (1 mL  $\times$  3). <sup>b</sup> Pretreatment of **TCO-C6-Cl** (50  $\mu\text{M}$ ) for 1 h, followed by washing with PBS (1 mL  $\times$  3).



**Table S10** Cellular uptake of complexes **1 – 4** by HeLa cells transfected with the pHTN HaloTag CMV-neo Vector.

Complex	Amount of iridium/fmol <sup>a</sup>		
	Complex only	+ <b>BCN-C6-Cl</b> <sup>b</sup>	+ <b>TCO-C6-Cl</b> <sup>c</sup>
<b>1</b>	0.489 ± 0.006	0.645 ± 0.012	0.641 ± 0.012
<b>2</b>	0.716 ± 0.010	1.159 ± 0.010	1.078 ± 0.006
<b>3</b>	0.742 ± 0.010	1.533 ± 0.007	1.406 ± 0.017
<b>4</b>	0.897 ± 0.007	1.976 ± 0.024	1.963 ± 0.025

<sup>a</sup> Amount of iridium of complexes **1 – 4** associated with an average HeLa cell upon incubation with the complexes (10 μM) at 37 °C for 1 h, as determined by ICP-MS. <sup>b</sup> Pretreatment of **BCN-C6-Cl** (50 μM) for 1 h, followed by washing with PBS (1 mL × 3). <sup>c</sup> Pretreatment of **TCO-C6-Cl** (50 μM) for 1 h, followed by washing with PBS (1 mL × 3).

**Fig. S1** Electronic absorption spectra of complexes **1** – **4** and bpy-Tz-Ph in CH<sub>2</sub>Cl<sub>2</sub> (black) and CH<sub>3</sub>CN (red) at 298 K.

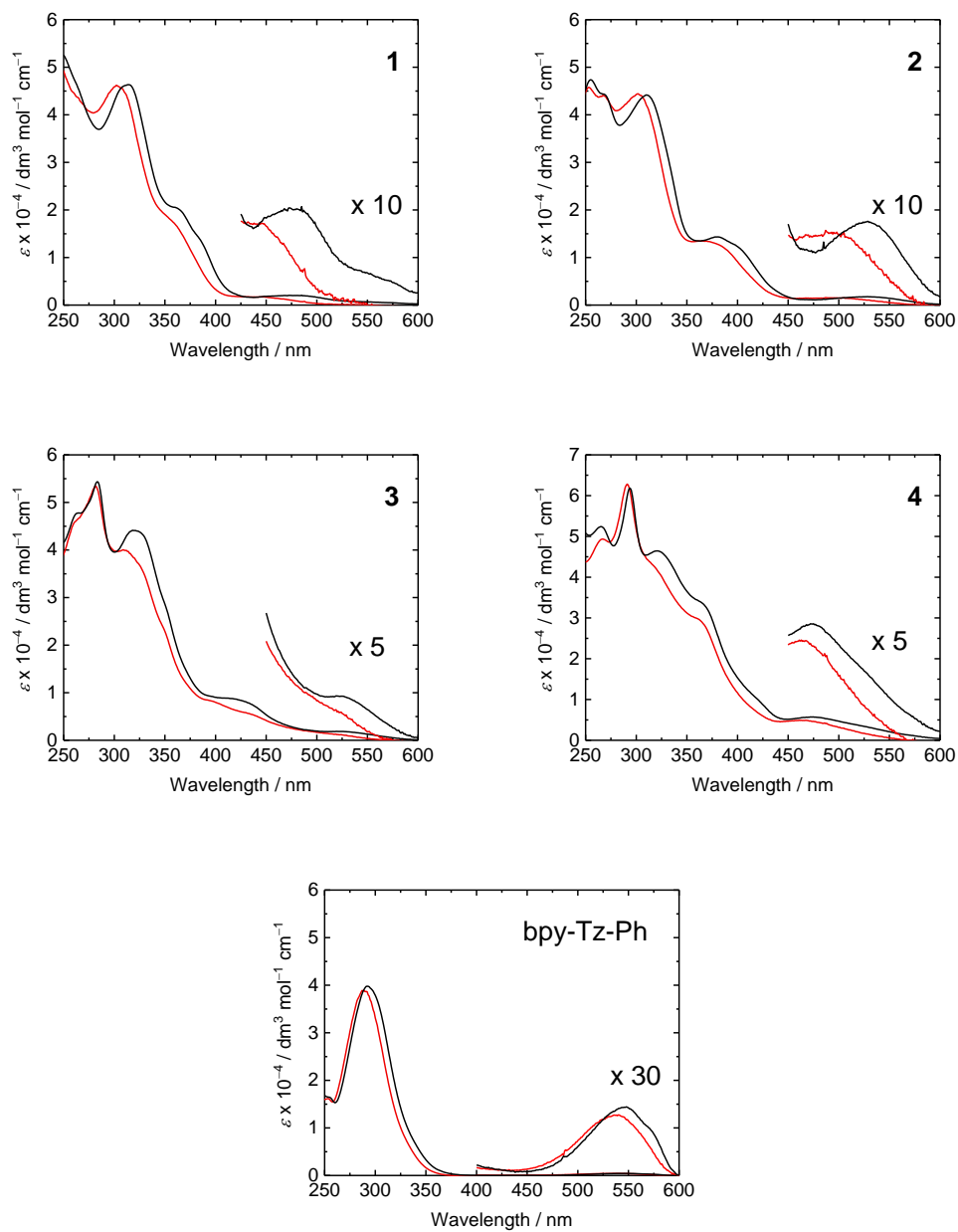


**Fig. S2** Emission spectra of complexes **1** – **4** in degassed  $\text{CH}_2\text{Cl}_2$  (black) and  $\text{CH}_3\text{CN}$  (red) at 298

K. Excitation wavelength = 350 nm.

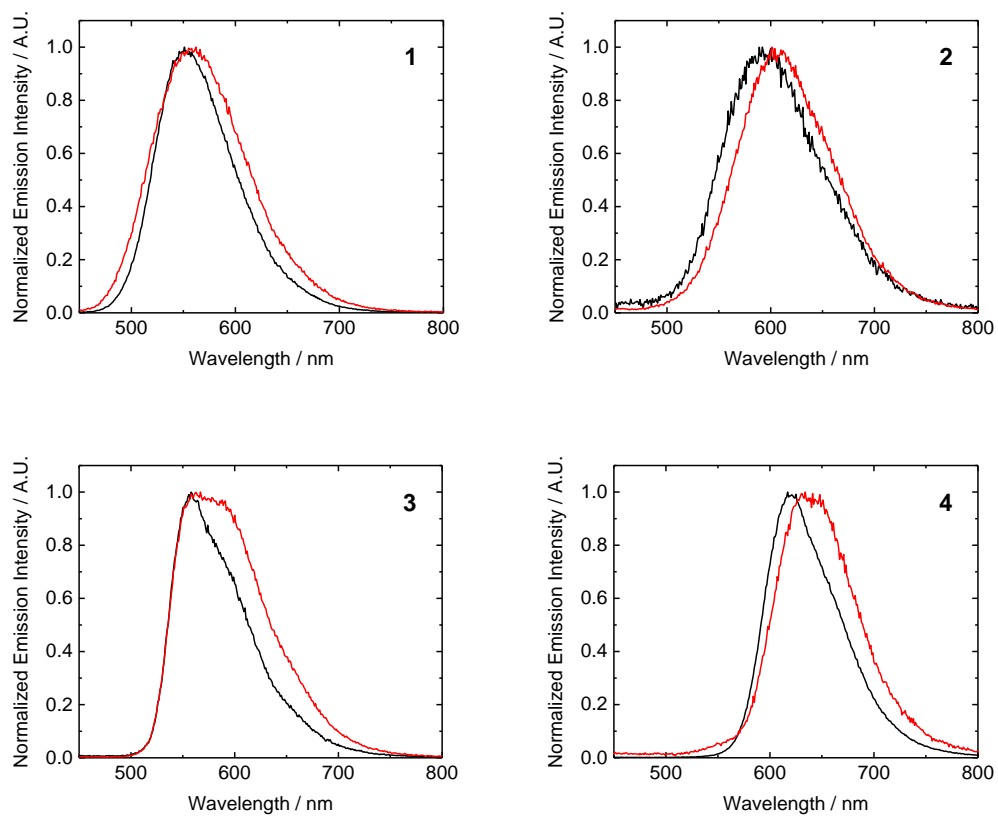


**Fig. S3** Relative absorbance of solutions of complexes **1 – 4** (black), **1a – 4a** (red) and **1b – 4b** (blue) (10  $\mu$ M) in aerated potassium phosphate buffer (50 mM, pH 7.4)/DMSO (99:1, v/v) at 298 K under continuous photoexcitation at 365 nm (1 mW/cm<sup>2</sup>).

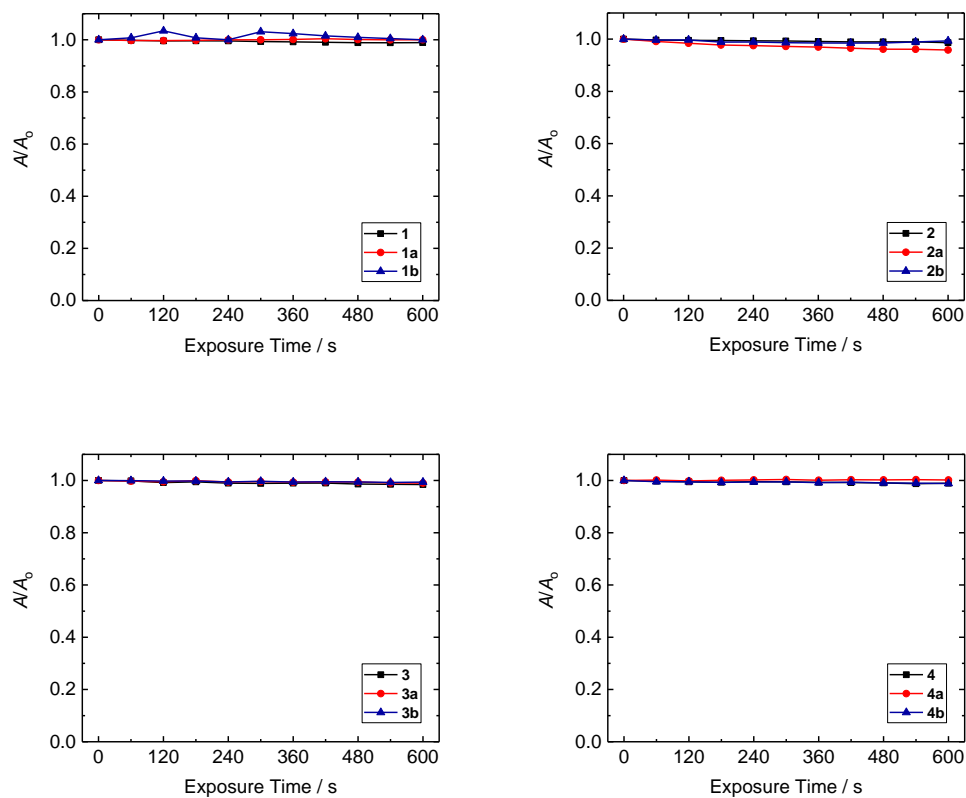


**Fig. S4** Relative emission intensities of solutions of complexes **1 – 4** (black), **1a – 4a** (red) and **1b – 4b** (blue) (10  $\mu$ M) in aerated potassium phosphate buffer (50 mM, pH 7.4)/DMSO (99:1, v/v) at 298 K under continuous photoexcitation at 365 nm (1 mW/cm<sup>2</sup>).

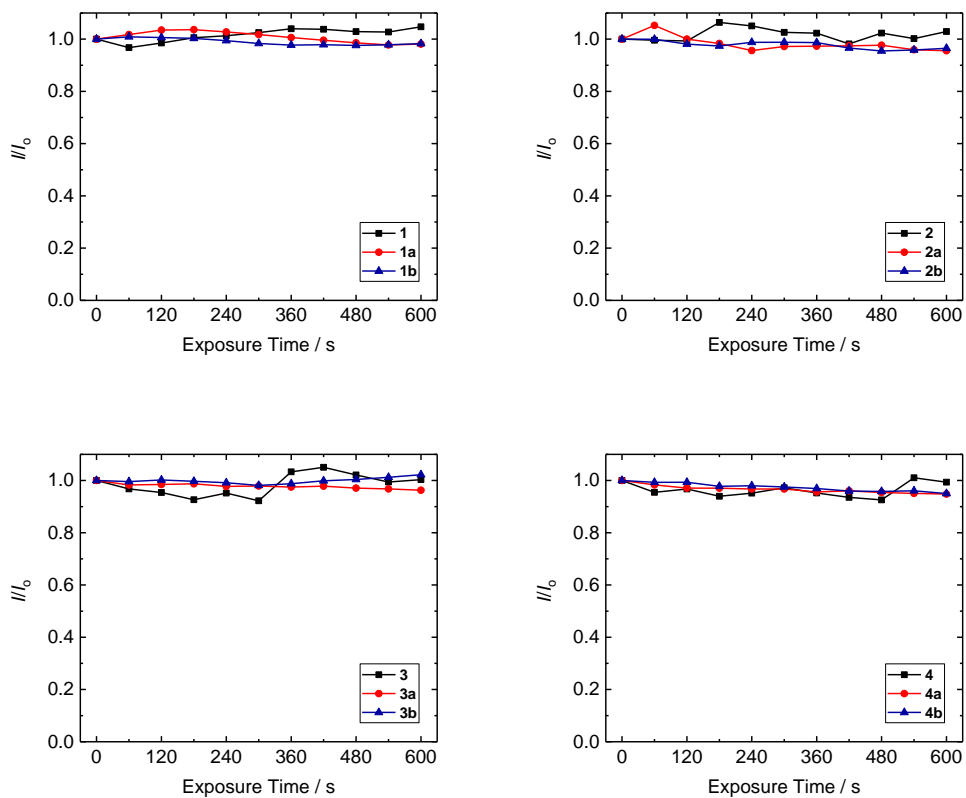
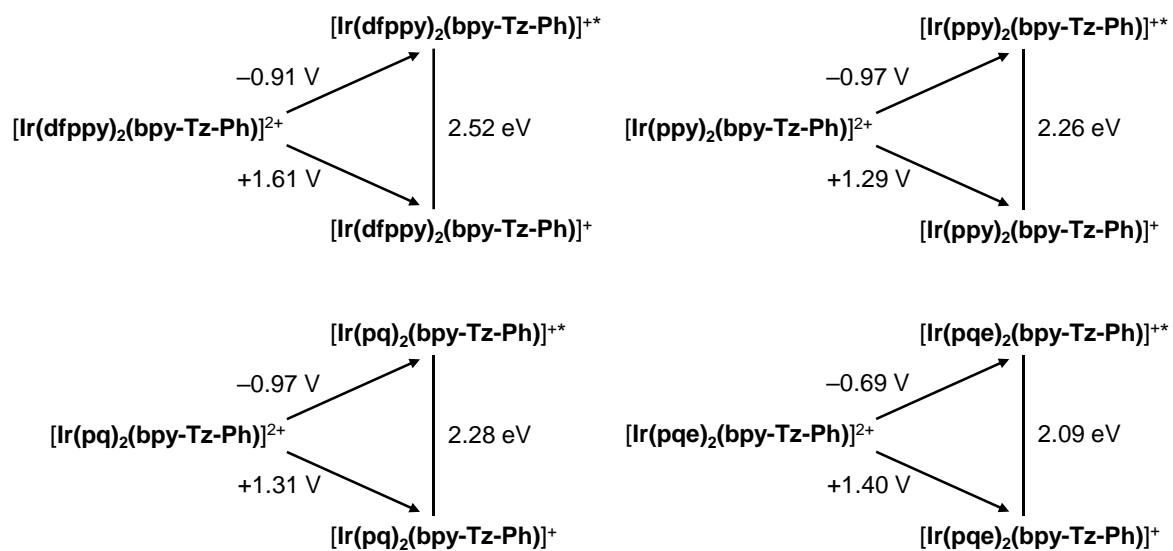
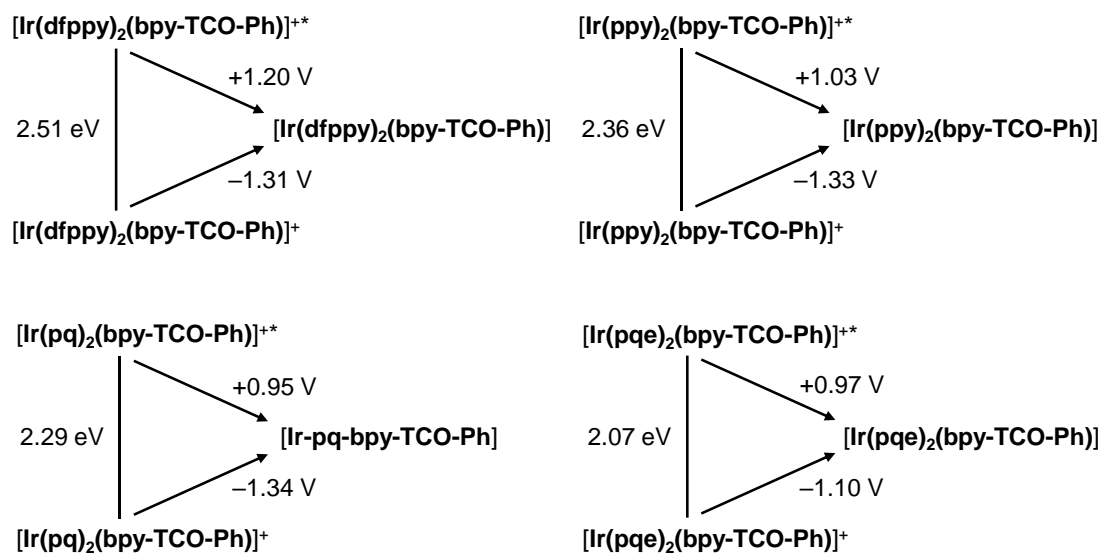


Fig. S5 Latimer diagrams showing the excited-state redox potentials of complexes 1 – 4.



**Fig. S6** Latimer diagrams showing the excited-state redox potentials of complexes **1b** – **4b**.



**Fig. S7** Spectral overlap of the absorption spectrum of the acceptor bpy-Tz-Ph and normalized emission spectrum of the donor complexes **1** – **4** in CH<sub>3</sub>CN at 298 K. The extinction coefficient of bpy-Tz-Ph was 425 M<sup>-1</sup> cm<sup>-1</sup> at 540 nm.

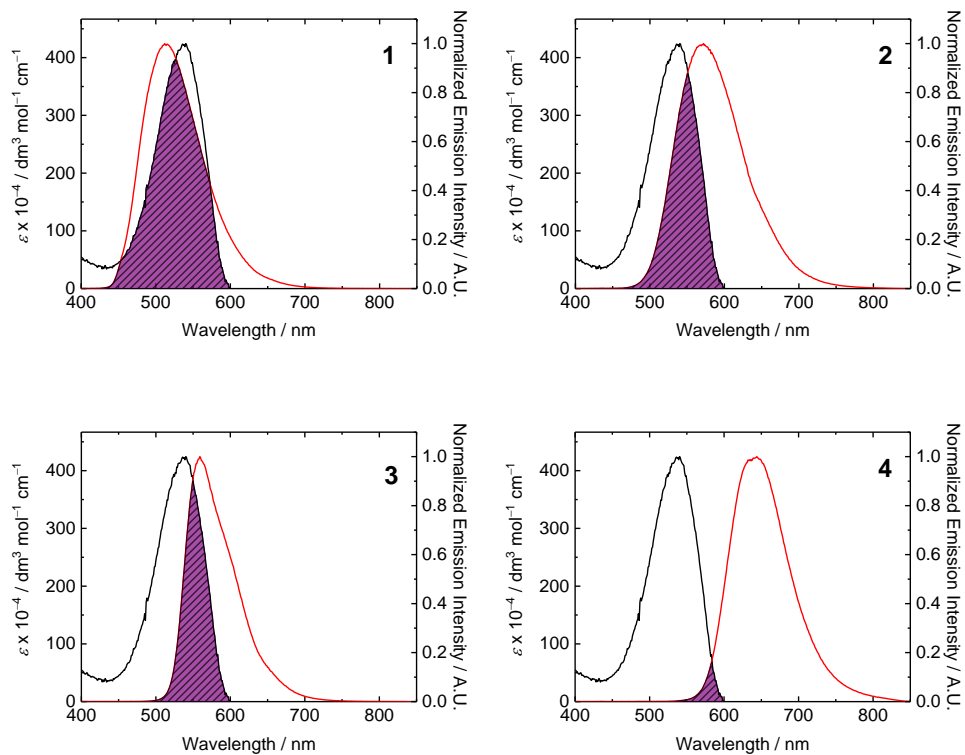




**Fig. S8** Pseudo first-order kinetics for the reactions of complexes **1** – **4** with **BCN-OH** at different concentrations in MeOH/H<sub>2</sub>O (1:1, v/v) at 298 K. The slope corresponds to the  $k_2$  of the reaction.

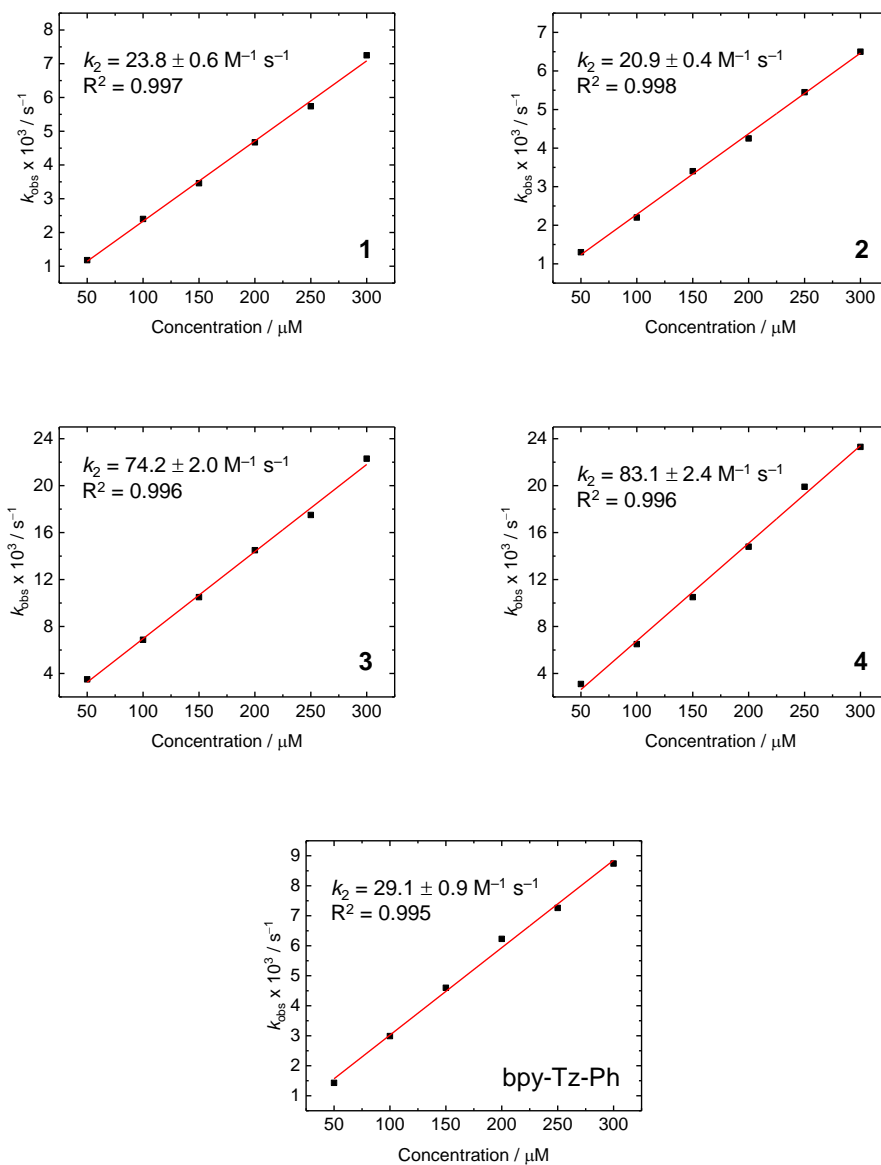


**Fig. S9** Pseudo first-order kinetics for the reactions of complexes **1** – **4** with TCO-OH at different concentrations in MeOH/H<sub>2</sub>O (1:1, v/v) at 298 K. The slope corresponds to the  $k_2$  of the reaction.

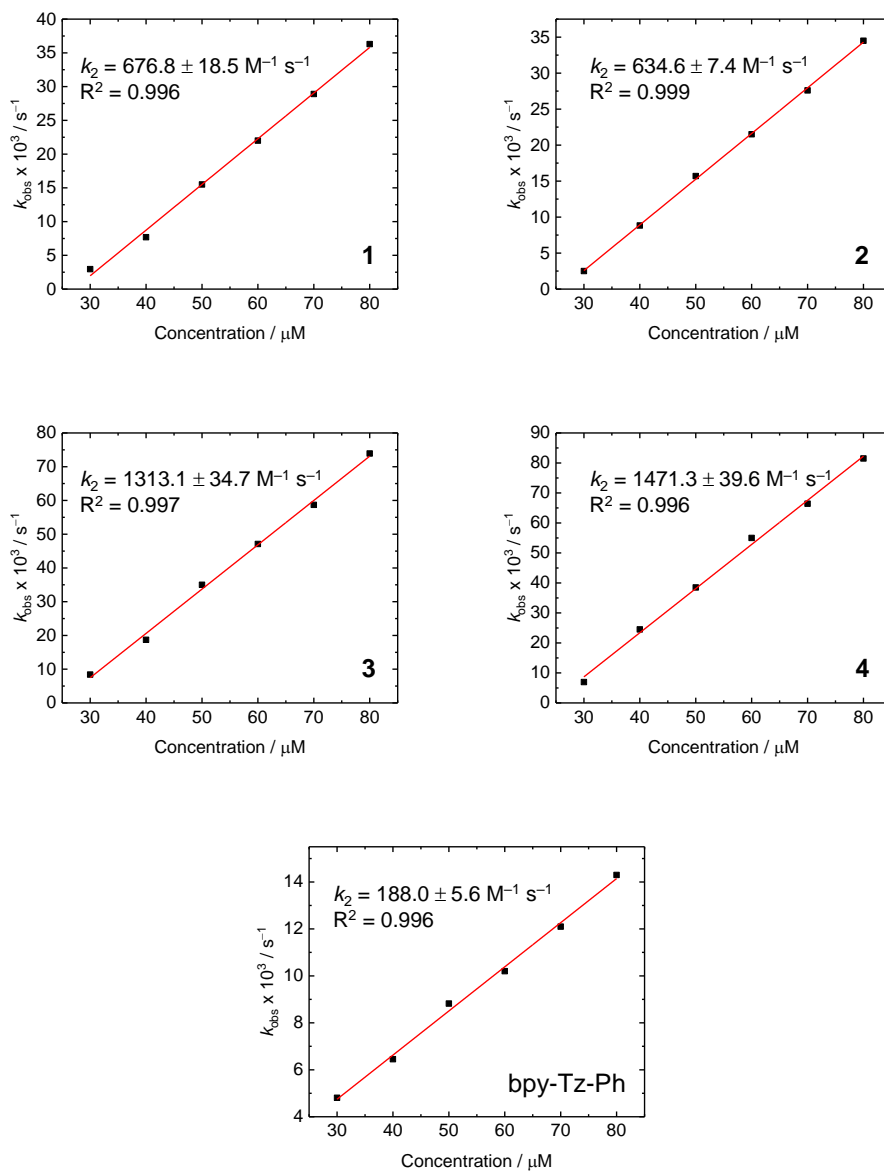


**Fig. S10** SDS-PAGE analysis of the reactions of complex **2** with **BCN-BSA** and **TCO-BSA**. Left: UV transillumination; right: Coomassie Blue staining. Lanes 1 and 4: complex with **BCN-BSA**; lanes 2 and 5: complex with **TCO-BSA**; lanes 3 and 6: complex with unmodified BSA.

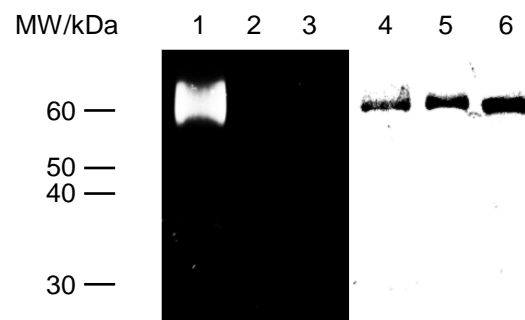


**Fig. S11** LSCM images of HeLa cells pretreated with **BCN-morph** (50  $\mu$ M, 2 h) and **BCN-DPPE** (50  $\mu$ M, 2h) and incubated with complex **2** (10  $\mu$ M, 2 h) at 37°C.

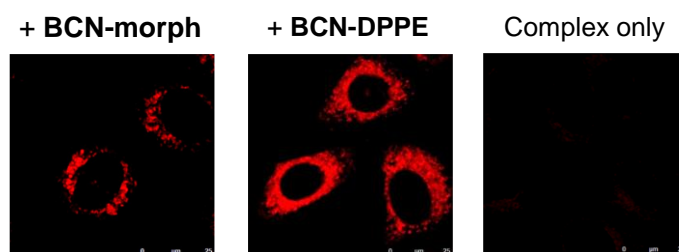
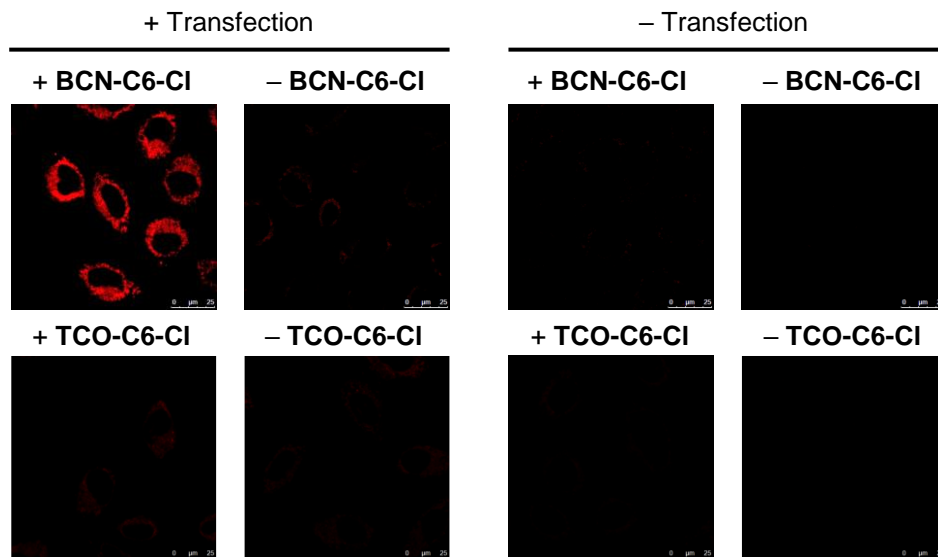


**Fig. S12** LSCM images of HeLa cells incubated with complex **2** (10  $\mu$ M) at 37°C for 1 h. Only cells expressing cytoplasm-enriched HaloTag with pretreatment of **BCN-C6-Cl** (50  $\mu$ M, 1 h) showed intense phosphorescence signal.



## References

- S1. D. D. Perrin and W. L. F. Armarego, *Purification of Laboratory Chemicals*, Elsevier, Oxford, U. K., 2009.
- S2. T. S.-M. Tang, K.-K. Leung, M.-W. Louie, H.-W. Liu, S. H. Cheng and K. K.-W. Lo, *Dalton Trans.*, 2015, **44**, 4945.
- S3. (a) S. Sprouse, K. A. King, P. J. Spellane and R. J. Watts, *J. Am. Chem. Soc.*, 1984, **106**, 6647; (b) F. O. Garces, K. A. King and R. J. Watts, *Inorg. Chem.*, 1988, **27**, 3464.
- S4. B. M. Peek, G. T. Ross, S. W. Edwards, G. J. Meyer, T. J. Meyer and B. W. Erickson, *Int. J. Pept. Protein Res.*, 1991, **38**, 114.
- S5. J. Shum, P.-Z. Zhang, L. C.-C. Lee and K. K.-W. Lo, *ChemPlusChem*, 2020, **85**, 1374.
- S6. H. E. Murrey, J. C. Judkins, C. W. am Ende, T. E. Ballard, Y. Fang, K. Riccardi, L. Di, E. R. Guilmette, J. W. Schwartz, J. M. Fox and D. S. Johnson, *J. Am. Chem. Soc.*, 2015, **137**, 11461.
- S7. J. N. Demas and G. A. Crosby, *J. Phys. Chem.*, 1971, **75**, 991.
- S8. N. Katsumi, *Bull. Chem. Soc. Jpn.*, 1982, **55**, 2697.
- S9. M. J. McKeage, S. J. Berners-Price, P. Galettis, R. J. Bowen, W. Brouwer, L. Ding, L. Zhuang and B. C. Baguley, *Cancer Chemother. Pharmacol.*, 2000, **46**, 343.
- S10. R. W. Redmond and J. N. Gamlin, *Photochem. Photobiol.*, 1999, **70**, 391.
- S11. A. A. Abdel-Shafi, P. D. Beer, R. J. Mortimer and F. Wilkinson, *J. Phys. Chem. A*, 2000, **104**, 192.